

УДК 616-006  
© Коллектив авторов, 2017

Li Peng<sup>1</sup>, Ildar R. Kabirov<sup>2</sup>, Valentin N. Pavlov<sup>2</sup>, Pengyu Guo<sup>1</sup>,  
Jiaqi Wang<sup>1</sup>, Dayong Hou<sup>1</sup>, Zhichao Wang<sup>1</sup>, Wei Zhang<sup>1</sup>, Wanhai Xu<sup>1</sup>  
**INTRAOPERATIVE NEAR-INFRARED IMAGING FOR PRECISE RESECTION  
OF BLADDER CANCER BY AVB3 TARGETING FLUORESCENT AGENT**

<sup>1</sup>Harbin Medical University  
<sup>2</sup>Bashkir State Medical University

Bladder cancer is one of the most common malignancies and contributes significantly to the overall human cancer burden. In order to solve the difficulties in the highly sensitive detection bladder cancer, detecting tumor residual and defining the margin of bladder tumor we use intraoperative fluorescence molecular imaging.

The study was to synthesize a targeting agent indocyanine green-arginine-glycine-aspartic acid which is integrin  $\alpha\beta_3$ -targeted, fast clearing near-infrared probes both in vitro and in vivo for bladder cancer Imaging-guided therapy. This targeted agent could be used for fast clearing hydrophilic near-infrared dye indocyanine green for detecting  $\alpha\beta_3$  receptor expressing tumor foci during operation and finishing imaging guided surgery, using preclinical in vivo mouse models. The indocyanine green was conjugated with the arginine-glycine-aspartic acid, the indocyanine green-arginine-glycine-aspartic acid was synthesized. The toxicity of indocyanine green-arginine-glycine-aspartic acid was measured by MTT assay.

The probes specificity was assessed in vitro and in vivo using the MB49 ( $\alpha\beta_3$  receptor high expressing) bladder cancer cell lines in mice models. Fast clearing Near-infrared probes conjugated with arginine-glycine-aspartic acid peptide targeting  $\alpha\beta_3$  receptor can be used for highly specific and sensitive detection of tumor lesions in vivo.

These preclinical findings with intraoperative optical imaging technique holds promise to offer more sensitive and accurate bladder cancer resection guidance and achieve better surgical outcomes in cancer patients.

**Key words:** Image-guided therapy, Near-infrared, Indocyanine green, Tumor targeting, Arginine-glycine-aspartic acid.

Bladder cancer (BC) is one of the most common malignancies and contributes significantly to the overall human cancer burden [1, 2]. In China, the incidence rate of BC reached 80.5 per 100,000 population and is still increasing [1]. Surgical intervention, such as transurethral resection (TUR) and radical cystectomy, is usually the first treatment for BC that has not spread to other parts of the body [3]. However, despite tremendous efforts have been made to optimize surgical strategies for better clinical outcomes, the recurrence rate of BC still remains high. The one-year recurrence rate is 15%-61%, and the five-year recurrence rate can reach up to 78% [4,5].

For early-stage non-muscle invasive BC (NMIBC), the minimally invasive cystoscopy guided TUR is preferred as the gold standard [4]. However, conventional white-light cystoscopy (WLC) suffers the difficulty in visualizing flat neoplasms and defining the exact margins of BC [6], which results in high risk of leaving tumor residual and high recurrence rate. Hexaminolevulinate (HAL) guided blue-light fluorescence cystoscopy (BLFC) has been confirmed for the increased detection of BC and reduced recurrence rates over WLC from long-term follow-up studies [7], but its false-positive rate is still 30% due to the low specificity of HAL [8]. Therefore, new fluorescent agents with high tumor specificity are highly desired for clinical practice in BC resection.

Recently, various near-infrared (NIR) fluorescent agents were reported in applications of

intraoperative imaging-guided tumor resection for both preclinical and clinical studies [9, 10]. The utilization of NIR spectrum (commonly defined as 650 to 900 nm) shows several inherent advantages for surgical guidance comparing with conventional visible light, such as high tissue penetration ability, no auto-fluorescence from normal tissue, high signal-to-background ratio, and no interference from operating room light [11-13]. Several studies demonstrated the NIR agent-based intraoperative imaging can effectively visualize micro-tumor foci with diameters less than 2 mm in liver cancer [14], breast cancer [15], ovarian cancer [16], etc. However, the NIR fluorescence imaging guided surgery for BC resection has not yet been deeply investigated.

In this study, we synthesized arginine-glycine-aspartic acid (RGD)-conjugated highly loaded indocyanine green (ICG) (ICG-RGD) as a small molecular fluorescent probe for tumor-specific intraoperative imaging in BC resection. RGD is a peptide ligand that specifically binds the integrin  $\alpha_v\beta_3$  [17, 18]. This integrin is overexpressed in various types of tumor [19-22] and plays a critical role in regulating tumor growth, metastasis, and angiogenesis [23, 24]. Therefore, it has been used as a molecular target for developing new tumor imaging approaches in clinical trials [25-27]. ICG is currently the one and only NIR fluorescent dye that is approved by the Food and Drug Administration (FDA) in both United States and China. The efficacy of the newly de-

veloped ICG-RGD was validated in subcutaneous and orthotopic BC models in mice using a special intraoperative NIR imaging system designed by our team (Fig. 1). The results revealed that the

ICG-RGD based NIR imaging strategy had a great promise in providing objective guidance to urological surgeons for precise resection of BC (Fig. 1).

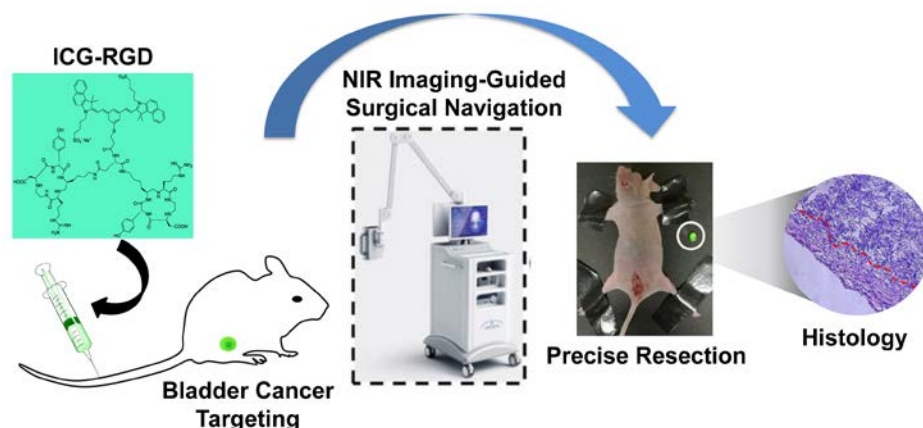


Fig. 1. A scheme showing the mechanism of ICG-RGD working in surgical navigation. ICG-RGD was synthesized and injected into the mice through tail vein. A home-made NIR guidance surgical navigation machine was applied to resect subcutaneous and orthotopic bladder tumor. The resected tissues were confirmed to be tumor tissues with negative tumor margin by histological analysis.

## Materials and Methods

### *Synthesis and characterisation of ICG -RGD*

We used EDC·HCl (2.8 mg) and NHS (1.5 mg.) in H<sub>2</sub>O (0.5 ml) to excited ICG (10 mg). At room temperature, stirring for 3 h in dark surroundings, the solution was mixed with appropriate RGD dissolved in sodium borate buffer. The mixture was stirred at room temperature overnight in the dark. The intermediate product ICG-NHS was first confirmed by thin layer chromatography (TCL) and the crude product ICG-RGD was subsequently purified by filtration. The absorbance and fluorescence spectra of ICG-RGD were recorded on a UV-vis spectrophotometer and an NIR spectral system. The photoluminescence quantum yields of RGD-based NIR probes were calculated as follows: where QY is the quantum yield of RGD-based NIR probes; QY<sub>s</sub> is the quantum yield of cypate; Au stand for the absorbance of cypate and RGD-based NIR probes at the excitation wavelength, respectively; and F<sub>s</sub>, F<sub>u</sub> are the integrated area of the cypate and RGD-based NIR probes under the fluorescence spectra, respectively. For stability analysis, the ICG-RGD (50 µg) was added to foetal bovine serum (FBS, 1 mL; Gibco, Australia), and its optical absorbance at 760 nm was monitored by UV-Vis spectroscopy (UV-2450; Shimadzu) at multiple time points for 48 h. An ICG in FBS control solution was also monitored for comparison.

### *Cell cytotoxicity assay*

MTT was used to evaluate the cellular cytotoxicity of ICG-RGD. MB49 (mouse urothelial carcinoma cell line) cells were seeded into 96 well plates 10000 cells/well in 200 µL cell culture medium. 24 h after attachment, cells were washed by PBS and the medium was replaced by fresh medi-

um with different concentration of ICG-RGD. 24 h after incubation, cells were washed by PBS prior to incubation with 0.5 mg/L MTT in 100 µL medium for 4 h. Then the supernatant was removed, the insoluble formazan crystals were dissolved in 200 µL dimethyl sulfoxide, the absorbance was measured using a microplate reader at a wavelength of 490 nm.

### *Mouse models bearing subcutaneous BC and in vivo fluorescence imaging*

All animals were purchased from the Vital River Laboratory Animal Technology Co. Ltd (China). All small animal experimental protocols were approved by the Institutional Animal Care and Ethics Committee of the Fourth Hospital of Harbin Medical University, and all the methods were carried out in accordance with the approved guidelines.

BALB/c nu/nu female mice (five weeks old) and mouse urothelial carcinoma cell line MB49 cells were used to establish the tumor xenografts. About  $2 \times 10^6$  MB49 cells in 75 µL DMED cell culture medium were injected into the elbow-back region of each mouse. Tumor growth was observed daily and checked by magnetic resonance imaging (MRI) until it was appropriate for in vivo experiments. Six mice with tumor size reached 5 mm in diameter were selected and divided into two groups. ICG and ICG-RGD probe (150 µL, 0.2 mg/mL for all mice) were injected intravenously (IV) into mice in the two groups, respectively. Then, in vivo fluorescence images were acquired at multiple time points (0 h, 0.5 h, 1 h, 2 h, 3 h, 6 h, 8 h, 12 h, 24 h, 36 h, 48 h) within the following 48 h using IVIS Spectrum Imaging System (PerkinElmer, USA) to access the ICG and ICG-RGD accumulation in tumors. For all imaging acquisitions, mice were anesthetized with a 3% isoflurane/air mixture.

### Orthotopic BC model establishment

Mice were anesthetized with sodium pentobarbital and catheterized with modified IV catheter (size: 24 G). Then, the inner surface of the bladder was successively washed by HCl and NaOH to induce minor damage of epithelium cells. After that, it was washed with phosphate-buffered saline (PBS) to eliminate residual NaOH. Finally, we infused 100  $\mu\text{L}$  ( $1 \times 10^7$ ) MB49 cells and incubated them in the bladder for 2 h.

### Magnetic resonance imaging

Diagnostic MRI scans (Aspect M3, Aspect Imaging, Israel) were performed to confirm the establishment tumor progression in BC mouse models. The input parameters were T1/T2 weighted spin echo sequences, slice thickness: 0.8-1mm, matrix: 256 $\times$ 256, window width: 19119, and window level: 9733.

### NIR fluorescence imaging-guide surgery and residual verification

Mice with subcutaneous and orthotopic tumor implantation were injected with ICG-RGD through their tail veins 8 h before surgery. Then, they were euthanized, and the tumors were removed by a urinary surgeon under the guidance of a home-made intraoperative NIR imaging system. During the operation, the tumor residual was illuminated and visualized in real time, and then

gradually resected until the surgeon considered that R0 resection was achieved. Harvested tissue was subjected to NIR fluorescence microscopy and histological examination.

### Statistics analysis

Data was analyzed using SPSS v.20 (IBM Software, USA). Data are presented as the means  $\pm$  standard deviations (SDs) for experiments performed in triplicate. Two-tailed, independent two-sample t-tests were used to assess differences in fluorescence intensities and tumor-to-background ratios between groups.  $P < 0.05$  indicated a significant difference.

### Results and discussion

#### Synthesis and characterisation of ICG-RGD

The chemical formula and simulated three-dimensional structure of the synthetic small molecule ICG-RGD is illustrated in Fig. 2A and B. The absorbance and fluorescence spectra analysis indicated that ICG-RGD exhibited similar absorption and excitation peaks as the ICG at around 778 nm and 822 nm (Fig. 2C), respectively. The photoluminescence quantum yield was the same as ICG. Furthermore, it demonstrated excellent stability in foetal bovine serum (Fig. 2D). The absorbance only dropped by less than 10% within 48 h of continuous observation.

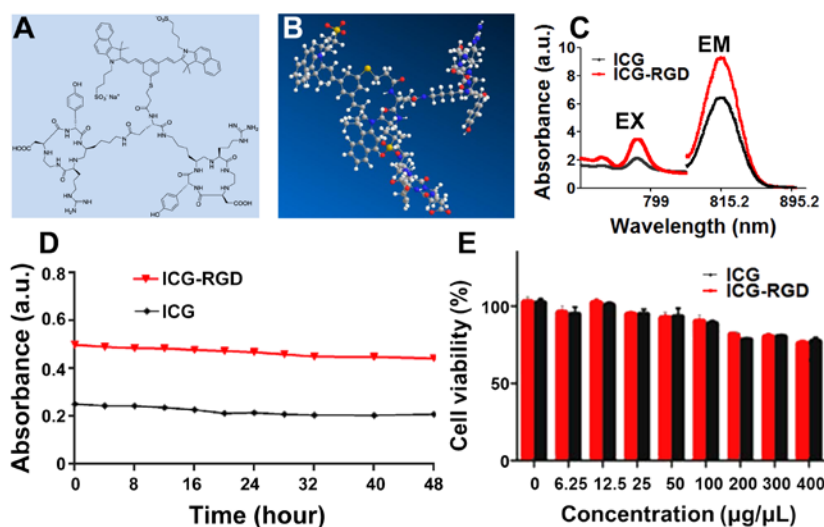


Fig. 2. Synthesis and characterisation of ICG-RGD. (A and B) The structure of ICG-RGD. (C) Visible absorption spectrum of ICG-RGD. (D) Absorbance at different time points. (E) MTT assay of ICG-RGD on MB49 cells at different time points.

### In vitro ICG-RGD cytotoxicity and uptake

MTT assay was performed to assess the ICG-RGD biocompatibility and ensure a safe dose that could be used in vivo. Fig. 2D demonstrates that ICG-RGD exhibited insignificantly different cytotoxicity comparing with ICG at all concentration levels ( $P > 0.05$ ), and the cell viability was still over 80% when the concentration reached 400  $\mu\text{g}/\text{mL}$ . This suggested that ICG-RGD had comparable biosafety as the FDA ap-

proved ICG and could be used safely for in vivo NIR imaging.

With the conjugation of RGD peptide, the proposed fluorescent probe was designed to have better tumor cell targeting capability than the conventional ICG. Through a fluorescence microscope, ICG-RGD was found to be internalized by mouse urothelial carcinoma MB49 cells (Fig. 3A-C), while ICG was internalized much less (Fig. 3D-F), which validated our expectation.

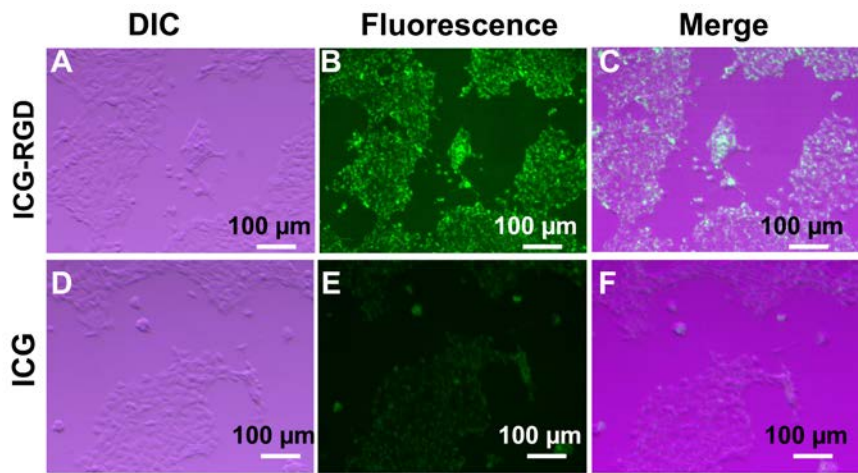


Fig. 3. DIC, fluorescent, and merged images after incubation with ICG-RGD (A-C) or ICG (D-F)

#### *In vivo fluorescence imaging and ICG-RGD biodistribution*

The subcutaneous BC-bearing nude mouse models were employed to validate the in vivo performance of ICG-RGD. Both T1 and T2 weighted MRI scans were performed as a diagnostic procedure for the tumor-bearing mice and

interpreted by an experienced radiologist and an urologist to ensure the model establishment was successful (Fig. 4A and B). Then, continuous fluorescence imaging was conducted in multiple observation of time-points to evaluate the tumor specificity of ICG-RGD in BC mouse models (Fig. 5).



Fig. 4. MRI identification of the subcutaneous tumor (A and B) or orthotopic bladder tumor (C and D)

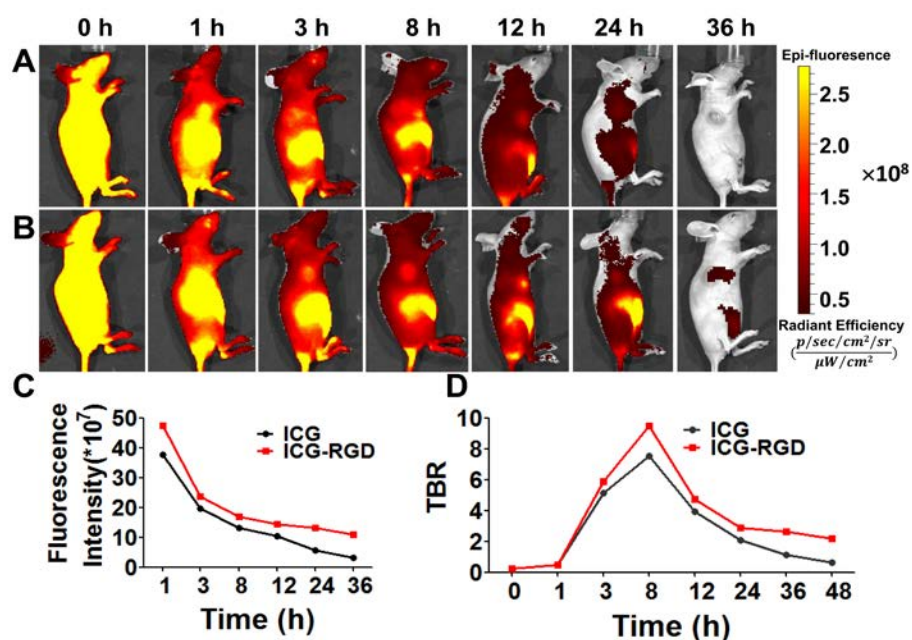


Fig. 5. In vivo fluorescence imaging and ICG-RGD biodistribution. (A-B) In vivo continuous observations (48 h) of bladder cancer xenografts after administration of ICG-RGD and ICG using IVIS. (C) Quantification of the fluorescence intensity at the tumour sites showing accumulation of ICG-RGD. (D) Comparison of TBR profiles of the two probes.

Figure 5A and B demonstrates that ICG-RGD exhibited better optical contrast in the tumor site (white arrows) than ICG from the 8 h time point onward. After the initial distribution period ( $< 3$  h), there was a relatively higher accumulation in the tumor and abdominal areas than the rest of the body for both ICG and ICG-RGD, but 8 h later, ICG was excreted gradually from the liver and digestive system as expected, whereas the retention time of ICG-RGD inside tumor was at least 12 h longer. The quantitative comparison also confirmed that ICG-RGD provided better signal intensity and greater tumor-to-background ratio (TBR) in the tumor comparing with ICG in all time points (Fig. 5C and D), which implied its superior in vivo BC targeting ability. These in vivo continuous observations also suggested that the best surgical window

would be 8 h post-injection, because the TBR profile reached its peak at this time (maximum TBR, ICG-RGD vs. ICG:  $9.9 \pm 0.8$  vs.  $7.5 \pm 0.7$ ,  $P < 0.05$ ).

Intraoperative BC resection in subcutaneous BC mouse models.

The feasibility of ICG-RGD was validated through NIR imaging-guided resection of BC in subcutaneous mouse models (Fig. 6). This process was conducted by using a home-made NIR imaging system (Fig. 1). The system was originally developed for the intraoperative navigation of sentinel lymph node (SLN) biopsy in breast cancer surgeries, which adopted ICG for pinpointing SLN during the operation [28]. Since the proposed ICG-RGD shared the similar excitation and emission spectra with ICG, the system was very suitable for BC surgeries using ICG-RGD.

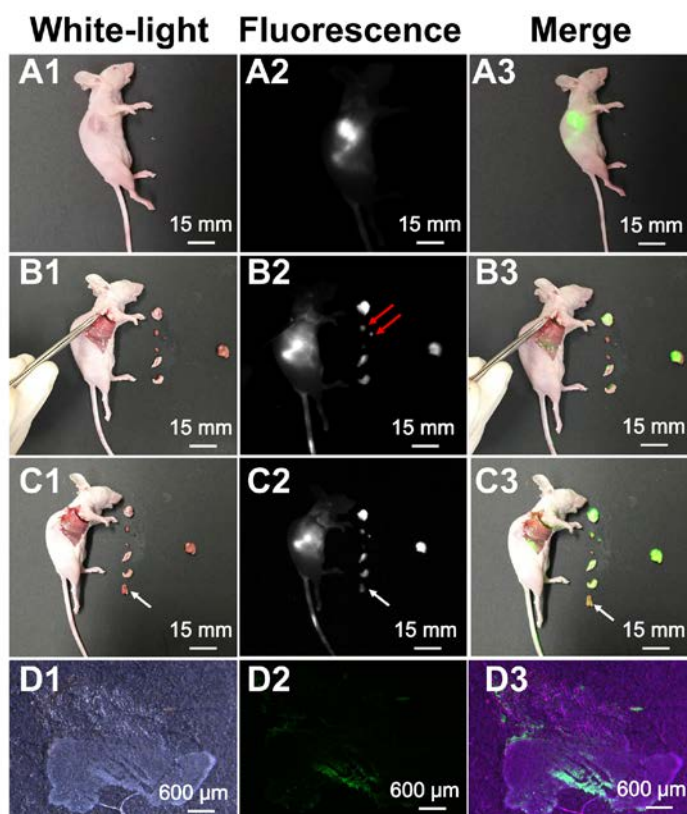


Fig. 6. Intraoperative tumor margin definition and tumor residual detection under NIR imaging guidance. (A1-A3) The tumor was illuminated with very high optical contrast. (B1-B3) the tumor tissue was gradually removed by the surgeon. The red arrow shows the residual tumor tissue between 1mm and 2mm. (C1-C3) All tumor residual was removed by a surgeon. The white arrow shows a residual tumor tissue pinpointed by the tweezers under the guidance of NIR imaging. (D1-D3) The excised tissue specimen was validated in the NIR fluorescence microscopy

Eight hours after the tail vein injection of ICG-RGD (0.2 mg/mL, 150  $\mu$ L), the tumor was illuminated with very high optical contrast (Fig. 6A1-A3). Then, the tumor tissue was gradually removed by the surgeon, and the excised pieces were placed right next to the mouse (Fig. 6B1-B3). Suspected residuals were effectively recognized during the operation, and those with the sizes between 1 mm to 2 mm can also be accurately located and resected (Fig. 6B2, red arrows). To

validate the accuracy of the tumor margin definition using ICG-RGD, the surgeon deliberately resected a piece of tissue containing both fluorescent and non-fluorescent regions (Fig. 6C1-C3, white arrows). Specimen slices were then taken from this tissue and observed under NIR fluorescence microscopy to identify the region with high ICG-RGD accumulation (Fig. 6D1-D3). After that, the high accumulation area was stained with H&E for histological analyses. Notably, there were also

fluorescence emitting from the abdominal part of the mouse after opening up the skin (Fig. 6B3 and C3), but they were likely to be the excreted ICG-RGD inside the intestine.

#### *Intraoperative BC resection in orthotopic BC mouse models*

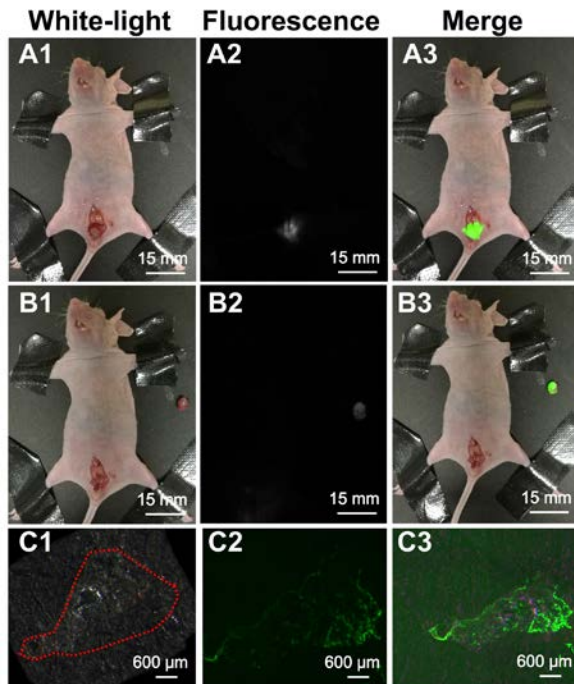


Fig. 7. Intraoperative detection of orthotopic MB49 bladder cancer under NIR imaging guidance. (A1-A3) NIR images exhibited an excellent optical contrast of the tumor. (B1-B3) The tumor tissue was removed under the imaging guidance (C1-C3). The excised tissue specimen was validated in the NIR fluorescence microscopy

NIR fluorescence imaging-guided BC surgery was also conducted in orthotopic mouse models. The mice were firstly scanned by MRI and interpreted by a radiologist and an urologist to verify the tumor growth in bladders (Fig. 4C and D). Then, their bladders were exposed 8 h post the IV injection of ICG-RGD (0.2 mg/mL, 150 $\mu$ L) (Fig. 7). Different from the subcutaneous tumor model, the orthotopic bladder tumor was far away from the liver and intestines, thus there was no interference of the fluorescent signal from the excreted ICG-RGD in the digestive system. The real-time NIR images exhibited an excellent optical contrast of the tumor (Fig. 7A1-A3), and the surgeon easily removed the tumor tissue under the imaging guidance (Fig. 7B1-B3). The excised tissue specimen was again validated in the NIR fluorescence microscopy (Fig. 7C1-C2), which clearly showed the distribution of ICG-RGD in the tissue.

#### **Histological analysis**

Frozen sections were deliberately obtained from the boundary regions between tumor and adjacent normal tissues indicated by NIR fluorescent images, and then stained with H&E. The results confirmed that the surgeon indeed found the tumor boundary in both subcutaneous (Fig. 8A and B) and orthotopic mouse models (Fig. 8C and D) under the guidance of NIR fluorescence imaging.

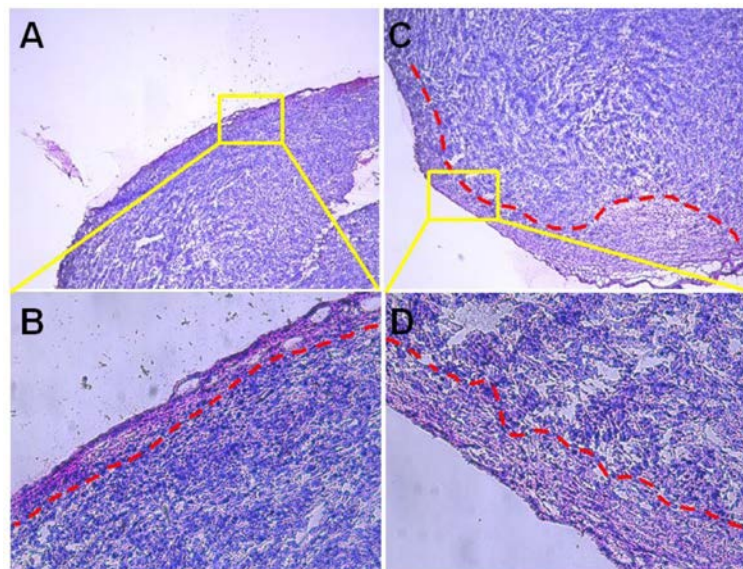


Fig. 8. Histological analysis of the resected tumor tissues. (A and B) HE staining of subcutaneous tumor tissue. (C and D) HE staining of orthotopic tumor tissue. Red dotted line means the tumor margin

In this study, we developed a NIR small molecule probe that conjugated RGD and ICG for tumor-specific intraoperative imaging in BC resection. The feasibility of the proposed ICG-RGD was evaluated through in vitro cellular and in vivo xenograft experiments. ICG-RGD based fluorescence imaging-guided surgeries were con-

ducted on subcutaneous and orthotopic mouse models, which demonstrated the efficacy of using the tumor targeting probe to achieve objective and accurate BC resection.

Optical imaging technologies have already been widely applied in BC surgeries. Conventional WLC and HAL based BLFC are both valu-

able clinical tools in minimally invasive TUR for NMIBC. However, randomized clinical trials and meta-analysis suggested that they still suffer from limited sensitivity and specificity in guiding surgeons to achieve precise BC resection [29-32], which is generally considered to be the reason of high postoperative recurrence rate. Therefore, we synthesized the ICG-RGD probe that combined the NIR fluorescent dye (ICG) for better sensitivity, as well as the integrin  $\alpha_v\beta_3$  receptor targeting peptide (RGD) for better specificity. Both components have been used in clinical applications, thus the proposed small molecule probe exhibited excellent biocompatibility and have great potential for clinical translations.

Comparing with ICG, ICG-RGD demonstrate improved tumor cell specificity (Fig. 3). The *in vivo* biodistribution imaging showed that the maximum TBR of using ICG-RGD was as high as  $9.9 \pm 0.8$ , which was significantly better than using ICG (Fig. 5). Furthermore, the intraoperative imaging-guided BC surgeries demonstrated that the proposed probe can effectively help surgeons to locate the tumor, define tumor margin, and continuously check whether there were tumor residuals during the operation. Because of the high sensitivity of NIR imaging, tumor micro-residuals with the size between 1 to 2 mm were successfully visualized and removed (Fig. 6), and this was achieved with the similar field of view as a clinical operation ( $15 \times 15 \text{ cm}^2$ ). All these revealed the benefits of using ICG-RGD in BC surgery and implied its great potential for clinical translations.

One more extra finding was that the excised tissues still exhibited great NIR fluorescence contrast between suspected tumor region and its adjacent normal tissue. This can also guide surgeons or pathologists to take out cryo-sections from the right location, rather than cutting specimens randomly for histology analysis. This may further save the operation time in real clinical applications. The NIR imaging system we employed in

this study was designed for open surgeries, but various endoscopic NIR imaging systems have been reported in treatment of different types of cancer [32-34]. The efficacy of using ICG-RGD and NIR fluorescence cystoscopy for TUR of BC in minimally invasive operation still needs sufficient instrumentation development and comprehensive *in vivo* investigations, which may be presented in our future studies.

### Conclusion

In conclusion, we construct a tumor specific probe, ICG-RGD, and demonstrate that it can effectively help surgeons to achieve precise resection of bladder tumor in animal models during NIR fluorescence imaging-guided surgeries. We believe this technique is promising and holds great potential for clinical translations in the future.

### Author contributions

Wanhai Xu conceived and designed the experiments; Li Peng, Ildar R. Kabirov, and Pengyu Guo performed the experiments; Dayong Hou, Wei Zhang and Valentin N. Pavlov contributed materials and analysis tools; Jiaqi Wang and Zhichao Wang analyzed the data; Li Peng, Ildar R. Kabirov wrote the paper.

### Acknowledgments

This work was supported by the National Natural Science Foundation of China under Grant Nos. 81270022, 81227901, 61231004, 81501540, 61671449, 61501462; the Strategic Priority Research Program from Chinese Academy of Sciences under Grant No. XDB02060010; the Beijing Municipal Science & Technology Commission under Grant No. Z161100002616022; Balb/c nude mice were purchased from Vital River Laboratory Animal Technology Co. Ltd (China). All small animal experimental protocols were approved by the Institutional Animal Care and Ethics Committee of the Fourth Hospital of Harbin Medical University, and all the methods were carried out in accordance with the approved guidelines.

### Authors:

**Li Peng** – PhD student of urology department of The Fourth Hospital of Harbin Medical University. Address: Harbin, Heilongjiang 150081, P. R. China. E-mail: 15636152446@163.com

**Ildar R. Kabirov** – PhD student of urology department of The Fourth Hospital of Harbin Medical University, assistant of Urology Department of Bashkir State Medical University. Address: 450008, Ufa, Lenina str., 3. E-mail: ildarkabirov@gmail.com.

**Valentin N. Pavlov** – Professor, Corresponding member of the Russian Academy of Sciences, President of Bashkir State Medical University. Address: 450008, Ufa, Lenina str., 3. E-mail: Pavlov@bashgmu.ru.

**Pengyu Guo** – PhD student of urology department of The Fourth Hospital of Harbin Medical University. Address: Harbin, Heilongjiang 150081, P. R. China. E-mail: guo\_peng\_yu@sina.com

**Jiaqi Wang** – MD student of urology department of The Fourth Hospital of Harbin Medical University. Address: Harbin, Heilongjiang 150081, P. R. China. E-mail: 346290658@qq.com

**Dayong Hou** – MD student of urology department of The Fourth Hospital of Harbin Medical University. Address: Harbin, Heilongjiang 150081, P. R. China. E-mail: 1301385343@qq.com

**Zhichao Wang** – PhD student of urology department of The Fourth Hospital of Harbin Medical University. Address: Harbin, Heilongjiang 150081, P. R. China. E-mail: wangzhch1987@126.com

**Wei Zhang** – MD student of urology department of The Fourth Hospital of Harbin Medical University. Address: Harbin, Heilongjiang 150081, P. R. China. E-mail: 1207920028@qq.com

**Wanhai Xu** – Professor, vice-president of The Fourth Hospital of Harbin Medical University, Chief of urology department of The Fourth Hospital of Harbin Medical University. Address: Harbin, Heilongjiang 150081, P. R. China. E-mail: xuwanhai@163.com

## REFERENCES

1. Chen W, Zheng R, Baade PD, Zhang S, Zeng H, Bray F, Jemal A, Yu XQ, He J: Cancer statistics in China, 2015. *Ca-cancer J Clin.* 2016, 66(2):115-132.
2. Voltaggio L, Cimino Mathews A, Bishop JA, Argani P, Cuda JD, Epstein JI, Hruban RH, Netto GJ, Stoler MH, Taube JM: Current concepts in the diagnosis and pathobiology of intraepithelial neoplasia: A review by organ system. *Ca-cancer J Clin.* 2016, 66(5):408-436.
3. Dalbagni G: Bladder cancer: Restaging TUR reduces recurrence and progression risk. *Nat. Rev. Urol.* 2010, 7(12):649-650.
4. Babjuk M, Burger M, Zigeuner R, Shariat SF, van Rhijn BW, Compérat E, Sylvester RJ, Kaasinen E, Böhle A, Palou RJ: EAU guidelines on non-muscle-invasive urothelial carcinoma of the bladder: update 2013. *Eur. Urol.* 2008, 54(2):303-314.
5. Pan Y, Volkmer JP, Mach KE, Rouse RV, Liu JJ, Sahoo D, Chang TC, Metzner TJ, Kang L, Van dRM: Endoscopic molecular imaging of human bladder cancer using a CD47 antibody. *SCI Transl. Med.* 2014, 6(260):e524.
6. Witjes JA, Moonen PM, Ag VDH: Comparison of hexaminolevulinate based flexible and rigid fluorescence cystoscopy with rigid white light cystoscopy in bladder cancer: results of a prospective Phase II study. *Eur. Urol.* 2005, 47(3):319-322.
7. Witjes JA, Redorta JP, Jacqmin D, Sofras F, Malmström PU, Riedl C, Jocham D, Conti G, Montorsi F, Arentsen HC: Hexaminolevulinate-Guided Fluorescence Cystoscopy in the Diagnosis and Follow-Up of Patients with Non-Muscle-Invasive Bladder Cancer: Review of the Evidence and Recommendations. *Eur. Urol.* 2010, 57(4):607-614.
8. a ASM, Hannes Penkoff MD, Elfriede Dajc-Sommerer MD, Andreas Zumbraegel MD, Lorenz Hoeltl MD, Michael Scholz MD, Claus Riedl MD, Josef Bugelnig MD, Alfred Hobisch MD, Maximilian Burger MD: Detection and clinical outcome of urinary bladder cancer with 5-aminolevulinic acid-induced fluorescence cystoscopy †. *Cancer* 2011, 117(5):938-947.
9. Saccomano M, Dullin C, Alves F, Napp J: Preclinical evaluation of near infrared (NIR) fluorescently labeled Cetuximab as a potential tool for fluorescence guided surgery. *Int. J Cancer* 2016, 139(10):2277-2289.
10. Vahrmeijer AL, Hutteman M, Jr VDV, Cj VDV, Frangioni JV: Image-guided cancer surgery using near-infrared fluorescence. *Nat. Rev. Clin. Oncol.* 2013, 10(9):507-518.
11. Garciaallende PB, Glatz J, Koch M, Tjalma JJ, Hartmans E, Symvoulidis P, Dam GMV, Nagengast WB, Ntziachristos V: Towards clinically translatable NIR fluorescence molecular guidance for colonoscopy. *Biomed. Opt. Express* 2014, 5(5):78-92.
12. Wada H, Hyun H, Vargas C, Gravier J, Park G, Gioux S, Frangioni JV, Henary M, Choi HS: Pancreas-Targeted NIR Fluorophores for Dual-Channel Image-Guided Abdominal Surgery. *Theranostics* 2015, 5(1):1.
13. Liang X, Shang W, Chi C, Zeng C, Wang K, Fang C, Chen Q, Liu H, Fan Y, Jie T: Dye-conjugated single-walled carbon nanotubes induce photothermal therapy under the guidance of near-infrared imaging. *Cancer Lett.* 2016, 383(2):243-249.
14. Zeng C, Shang W, Wang K, Chi C, Jia X, Fang C, Yang D, Ye J, Fang C, Tian J: Intraoperative Identification of Liver Cancer Microfoci Using a Targeted Near-Infrared Fluorescent Probe for Imaging-Guided Surgery. *Sci. Rep.* 2016, 6:21959.
15. Hill TK, Kelkar SS, Wojtynek NE, Soucek JJ, Payne WM, Stumpf K, Marini FC, Mohs A: Near Infrared Fluorescent Nanoparticles Derived from Hyaluronic Acid Improve Tumor Contrast for Image-Guided Surgery. *Theranostics* 2016, 6(13):2314-2328.
16. Lee JY, Thawani JP, Pierce J, Zeh R, Martinez-Lage M, Chanin M, Venegas O, Nims S, Learned K, Keating J: Intraoperative Near-Infrared Optical Imaging Can Localize Gadolinium-Enhancing Gliomas During Surgery. *Neurosurgery* 2016, 79(6):1.
17. Chen H, Niu G, Wu H, Chen X: Clinical Application of Radiolabeled RGD Peptides for PET Imaging of Integrin  $\alpha v \beta 3$ . *Theranostics* 2016, 6(1):78-92.
18. Wang Y, Xiao W, Zhang Y, Meza L, Tseng H, Takada Y, Ames JB, Lam KS: Optimization of RGD containing cyclic peptides against  $\alpha v \beta 3$  integrin. *Mol. Cancer Ther.* 2016, 15(2), 232-240.
19. Leblanc R, Lee SC, David M, Bordet JC, Norman DD, Patil R, Miller D, Sahay D, Ribeiro J, Clézardin P: Interaction of platelet-derived autotaxin with tumor integrin  $\alpha v \beta 3$  controls metastasis of breast cancer cells to bone. *Blood* 2014, 124(20):3141-3150.
20. Lópezrodríguez V, Galinosarco C, Garcíapérez FO, Ferroflores G, Arrieta O, MÁ Á: PET-Based Human Dosimetry of the Dimeric  $\alpha v \beta 3$  Integrin Ligand  $^{68}\text{Ga}$ -DOTA-E-[c(RGDfK)]<sub>2</sub>, a Potential Tracer for Imaging Tumor Angiogenesis. *J Nucl. Med.* 2015, 57(3).
21. Oudart JB, Doué M, Vautrin A, Brassart B, Sellier C, Dupontdeshorgue A, Monboisse JC, Maquart FX, Brassartpasco S, Ramont L: The anti-tumor NC1 domain of collagen XIX inhibits the FAK/ PI3K/Akt/mTOR signaling pathway through  $\alpha v \beta 3$  integrin interaction. *Oncotarget* 2015, 7(2):1516-1528.
22. Ma P, Yu H, Zhang X, Mu H, Chu Y, Ling N, Xing P, Wang Y, Sun K: Increased Active Tumor Targeting by An  $\alpha v \beta 3$ -Targeting and Cell-Penetrating Bifunctional Peptide-Mediated Dendrimer-Based Conjugate. *Pharm. Res.* 2016, 34(1):1-15.
23. Schnell O, Krebs B, Wagner E, Romagna A, Beer AJ, Grau SJ, Thon N, Goetz C, Kretzschmar HA, Tonn JC: Expression of integrin  $\alpha v \beta 3$  in gliomas correlates with tumor grade and is not restricted to tumor vasculature. *Brain Pathol.* 2008, 18(3):378-386.
24. Lorgner M, Hynes RO: Activation of Tumor Cell Integrin  $\alpha v \beta 3$  Controls Angiogenesis and Metastatic Growth in the Brain. *P. Natl. Acad. Sci. USA* 2009, 106(26):10666-10671.
25. Schmieder AH, Winter PM, Williams TA, Allen JS, Hu G, Zhang H, Caruthers SD, Wickline SA, Lanza GM: Molecular MR imaging of neovascular progression in the Vx2 tumor with  $\alpha v \beta 3$ -targeted paramagnetic nanoparticles. *Radiology* 2013, 268(2):470-480.
26. Terry SY, Abiraj K, Frielink C, van Dijk LK, Bussink J, Oyen WJ, Boerman OC: Imaging integrin  $\alpha v \beta 3$  on blood vessels with  $^{111}\text{In}$ -RGD2 in head and neck tumor xenografts. *J Nucl. Med.* 2014, 55(2):281.
27. Wenk CH, Ponce F, Guillermet S, Tenaud C, Boturyn D, Dumy P, Watrelot-Virieux D, Carozzo C, Josserand V, Coll JL: Near-infrared optical guided surgery of highly infiltrative fibrosarcomas in cats using an anti- $\alpha v \beta 3$  integrin molecular probe. *Cancer Lett.* 2013, 334(2):188.
28. Chi C, Zhang Q, Mao Y, Kou D, Qiu J, Ye J, Wang J, Wang Z, Du Y, Tian J: Increased precision of orthotopic and metastatic breast cancer surgery guided by matrix metalloproteinase-activatable near-infrared fluorescence probes. *Sci. Rep.* 2015, 5(4):562-564.
29. Daneshmand S, Schuckman AK, Bochner BH, Cookson MS, Downs TM, Gomella LG, Grossman HB, Kamat AM, Konety BR, Lee CT: Hexaminolevulinate blue-light cystoscopy in non-muscle-invasive bladder cancer: review of the clinical evidence and consensus statement on appropriate use in the USA. *Nat Rev. Urol.* 2014, 11(10):589-596.
30. Witjes JA, Babjuk M, Gontero P, Jacqmin D, Karl A, Kruck S, Mariappan P, Palou RJ, Stenzl A, Van VR: Clinical and Cost Effectiveness of Hexaminolevulinate-guided Blue-light Cystoscopy: Evidence Review and Updated Expert Recommendations. *Eur. Urol.* 2014, 66(5):863-871.
31. Liu JJ, Droller MJ, Liao JC: New Optical Imaging Technologies for Bladder Cancer: Considerations and Perspectives. *J Urology* 2012, 188(2):361.
32. Kosaka N, Mitsunaga M, Longmire MR, Choyke PL, Kobayashi H: Near infrared fluorescence-guided real-time endoscopic detection of peritoneal ovarian cancer nodules using intravenously injected indocyanine green. *Int. J Cancer* 2011, 129(7):1671-1677.
33. Ali T, Choyke PL, Kobayashi H: Endoscopic molecular imaging of cancer. *Future Oncol.* 2015, 9(10):1501-1513.
34. Tummers QR, Verbeek FP, Prevoo HA, Braat AE, Baeten CI, Frangioni JV, Cj VDV, Vahrmeijer AL: First experience on laparoscopic near-infrared fluorescence imaging of hepatic uveal melanoma metastases using indocyanine green. *Surg. Innov.* 2014, 22(1):20-25.